Correlative ^{201}Tl SPECT, MRI and Ex Vivo ^{201}Tl Uptake in Detecting and Characterizing Cervical Lymphadenopathy in Head and Neck Squamous Cell Carcinoma

Renato A. Valdés Olmos, Wim Koops, Barbara M. Loftus, Ing H. Liem, Reinhold T. Gregor, Cornelis A. Hoefnagel, Frans J. M. Hilgers and Alfons J. M. Balm

Departments of Nuclear Medicine, Diagnostic Radiology, Pathology and Otolaryngology/Head and Neck Surgery, The Netherlands Cancer Institute, Amsterdam, The Netherlands

The value of SPECT with ^{201}Tl chloride, in combination with MRI (particularly short inversion-time inversion recovery [STIR] sequences that suppress fat signals) to detect and characterize cervical lymphadenopathies (nodes ≥ 1 cm), and ex vivo lymph node ^{201}Tl uptake were studied in patients with squamous cell carcinoma of the head and neck. **Methods:** Preoperative SPECT and MRI, displayed in similar planes, were compared with the histologic findings in 15 neck dissection specimens from 12 patients with squamous cell carcinoma of the head and neck (9 with unilateral and 3 with bilateral neck dissection). Results were evaluated topographically with regard to the lymph node compartments (levels) of the neck. In addition, in 8 of these patients, the ^{201}Tl activity of dissected lymph nodes of 10 neck sides was measured immediately after surgery in a gamma counter and expressed as percentage of the injected dose per gram tissue (%ID/g). **Results:** Sixty-two lymph node levels were evaluated histologically. The high sensitivity of MRI (92% versus 71% for ^{201}Tl SPECT), which correctly detected lymph node involvement in 22 of 24 levels, and the high specificity of ^{201}Tl SPECT (92% versus 71% for MRI), which correctly characterized as negative 35 of 38 lymph node levels without metastasis on histology, led to a combined ^{201}Tl SPECT/MRI accuracy of 92%. ^{201}Tl SPECT was particularly effective in excluding involvement in 9 tumor-free neck levels with pathologically enlarged lymph nodes on MRI but failed to confirm involvement in 5 other tumor-positive levels. Mean ^{201}Tl uptake in 53 lymph nodes with confirmed histologic involvement was significantly higher than uptake in 145 tumor-free lymph nodes (0.0043 ± 0.0022 %ID/g versus 0.0023 ± 0.0014 %ID/g, $P = 0.0001$), muscle and fat tissue but clearly lower than salivary gland uptake. **Conclusion:** Although ^{201}Tl SPECT is not sensitive enough to be used as an independent imaging modality for staging of the neck, its correlative application with MRI appears to be an accurate method for the assessment of regional spread in head and neck squamous cell carcinoma. The ability of ^{201}Tl SPECT to characterize neck lymphadenopathies detected by MRI appears to be based on the difference in ^{201}Tl concentration found in lymph nodes with and without tumor involvement.

Received Jul. 22, 1998; revision accepted Mar. 5, 1999.

For correspondence or reprints contact: Renato A. Valdés Olmos, MD, Department of Nuclear Medicine, The Netherlands Cancer Institute, Plesmanlaan 121, 1066 CX Amsterdam, The Netherlands.

Key Words: SPECT; ^{201}Tl chloride; MRI; neck metastases; squamous cell carcinoma

J Nucl Med 1999; 40:1414–1419

The assessment of cervical lymph node metastases in patients with squamous cell carcinoma of the head and neck is essential for the clinical management of the disease. Staging of the neck, which constitutes a diagnostic problem because of the large number of lymph nodes located in this area (*1*), determines the extent of treatment modalities such as surgery or radiotherapy. In addition to palpation, staging of the neck increasingly relies on imaging modalities such as CT and MRI that use lymph node size and central lucency as criteria for detection of metastatic disease (*2–4*). Although lymph nodes ≥ 10 mm in diameter are generally considered to be positive (*5*), lymph node enlargement may also be the result of reactive and inflammatory processes that may limit the accuracy of CT and MRI. Moreover, detection of micrometastases in small nodes still remains a difficult issue (*6,7*).

To overcome these limitations, ultrasound-guided fine-needle aspiration cytology (USG-FNAC) was introduced in recent years. By combining detection by sonography with tissue characterization by microscopy (*8,9*), this technique has reached high accuracy levels in the diagnosis of regional spread in clinically negative necks and necks with lymphadenopathies. However, the accuracy of USG-FNAC depends on the skill of the sonographer and the cytopathologist, and the technique requires multiple aspirations. As an alternative modality, PET has been used for the staging of the neck. ^{18}F-fluorodeoxyglucose (FDG) is able to detect metastases measuring 4 mm or more, but the relatively high false-positive rate caused by uptake in reactive lymph nodes (*10*) has led to the use of other compounds, such as L-[^{11}CH3]-methionine (*11*) and L-1-[^{11}C]-tyrosine (*12,13*), that appear to be more accurate in differentiating cancerous from inflammatory cells.

The effectiveness of SPECT with ^{201}Tl-chloride to exclude neck lymph node involvement in patients with various head and neck malignancies in a previous study (*14*) led us to test the method in the characterization of cervical lymphadenopathies already detected by MRI in patients with head and neck squamous cell carcinoma to ascertain its value in staging the neck. In the previous study, the accuracy of ^{201}Tl SPECT was determined only on the basis of data recorded per dissected neck side. However, this study includes a topographical analysis considering six neck levels per neck side to complete the evaluation of the test in staging the neck. Finally, on the basis of correlative ex vivo lymph node ^{201}Tl uptake measurements and histologic findings, this study evaluates differences in lymph nodes with and without tumor involvement.

MATERIALS AND METHODS

Patients

Twelve consecutive patients (6 men, 6 women; age range 44–73 y; mean age 61.8 y) with histologically confirmed head and neck squamous cell carcinoma, scheduled for neck dissection, were included in the study after having provided informed consent. Clinical assessment was performed by the head and neck surgeon; subsequently, patients underwent MRI and ^{201}Tl SPECT. In 8 patients, ^{201}Tl-chloride was administered on the day of surgery to enable ex vivo lymph node counting after neck dissection and comparison with histologic findings. Classification of the primary tumor and neck lymph nodes was based on the TNM system of the Union Internationale Contre le Cancer (UICC, 1992). Clinical data of patients are summarized in Table 1. Neck dissection was unilateral in 9 patients and bilateral in 3 patients, which resulted in a total of 15 evaluated neck sides.

^{201}Tl Imaging

SPECT acquisition was performed according to a standardized method of fixation to prevent head movements and to obtain a position similar to MRI. SPECT studies were performed with a Vertex dual-head gamma camera (ADAC, Milpitas, CA) equipped with low-energy, high-resolution collimators 60 min after intravenous injection of 150 MBq (4 mCi) ^{201}Tl-chloride. Acquisition was based on 360° noncircular rotation, 6° step angles, 60 s per frame, 64 × 64 × 16 matrix and a zoom factor of 1.85 (pixel size 5 mm). Reconstruction was performed with Butterworth filter (order 5, cutoff 0.35); reorientation of images was performed following planes similar to the MR images, with sagittal, coronal and transverse one-pixel slices and additional three-dimensional volume reconstruction to identify tumor sites with exact documentation of the region and neck level.

MRI

MR images (T1- and T2-weighted pulse sequences with transaxial and sagittal slices of 3- to 5-mm thickness, field of view 200–250 cm, 256 × 256 matrix) were obtained with a Siemens Magnetom 63 SP4000 (Erlangen, Germany) 1.5-T scanner before and after intravenous administration of gadolinium diethylenetriaminepentaacetic acid. In addition, coronal short inversion-time inversion recovery (STIR) sequences, which suppress fat signals, were obtained with a slice thickness of 5 mm.

Histologic Preparation and Ex Vivo ^{201}Tl Lymph Node Uptake Measurements

After neck dissection lymph nodes and normal tissues were prepared by the pathologist, and lymph nodes per neck level were precisely localized in the specimen. Subsequently, after meticulous excision from the specimen, all lymph nodes received identification labels. For ex vivo ^{201}Tl uptake measurements, lymph nodes and normal tissues were placed in single well-identified counting tubes and were weighed and measured in a gamma well counter. Data were corrected for decay and converted to percentage of the injected dose per gram tissue (%ID/g). After counting, lymph nodes were fixed, sectioned and stained routinely with hematoxylin and eosin. Multiple levels were examined microscopically for the presence of tumor.

Analysis

Sensitivity, specificity and accuracy were calculated for each imaging modality and for the combination of both methods. MR

TABLE 1
Patient Characteristics, Tumor/Treatment Data, Histology and Imaging Results per Neck Side

Patient no.	Sex	Age (y)	Tumor location (staging)	Neck dissection (side)	Histology R/L	^{201}Tl SPECT R/L	MRI R/L
1	M	56	Oropharynx (recurrence)	RND (R)	+	+	+
2	F	73	Oropharynx (T3N2b)	RND (R)	+	+	+
3	M	59	Oropharynx (T3N2)	RND (R)	+	+	+
4	F	67	Larynx (T2N2c)	RND (R/L)	+/+	+/+	+/+
5	F	72	Esophagus (tongue metastasis)	SOND (R)	−	+	−
6	M	61	Oropharynx (T2N3)	RND (R)	+	+	+
7	M	44	Maxilla	SOND (R)	+	+	+
				RND (L)	+	+	+
8	F	60	Oropharynx (T3N0)	RND (R)	−	−	+
9	F	60	Larynx (T3N2)	MRND (R)	−	−	+
				RND (L)	+	+	+
10	F	59	Hypopharynx (T3N1)	MRND (R)	+	+	+
11	M	59	Oropharynx (T2N2)	MRND (L)	+	+	+
12	M	63	Larynx (T3N0)	RND (R)	−	+	+

RND = radical neck dissection; + = positive; SOND = supraomohyoid neck dissection; − = negative; MRND = modified radical neck dissection.

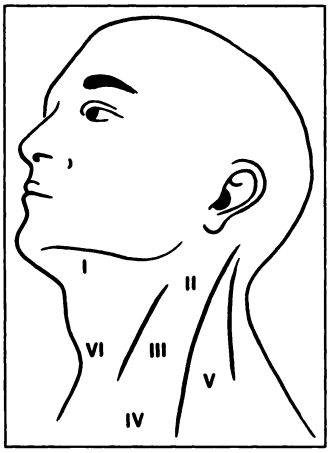

FIGURE 1. Lymph node groups divided into six levels per neck side according to Robbins et al. (*15*). Level I includes submental and submaxillary nodes; levels II/III/IV, jugular chain nodes; and level V, lymph nodes localized posteriorly to posterior border of sternocleidomastoid muscle. Level VI includes juxtavisceral lymph nodes.

and SPECT images were independently evaluated by two specialists in head and neck radiology and nuclear medicine. Examiners were unaware of the results of histology. Concerning SPECT, tumor uptake, visually assessed using a four-step score taking background activity of the neck as reference, was scored as intense (++), moderate (+), weakly positive (±) or absent (−); only intense and moderate were considered conclusive for pathology. With respect to MRI, on T1- and T2-weighted pulse sequences, lymph nodes with a diameter ≥ 10 mm and nodes that showed irregular enhancement and that were surrounded by a rim of enhancing viable tumor or lymph node tissue were classified as positive, according to well-established criteria (*5*); on coronal STIR sequences only lymph node size ≥ 10 mm was used as a pathologic criterion. For topographical evaluation, the findings of SPECT and MRI were recorded according to a standardized classification (*15*) that divides each neck side into six levels (Fig. 1). Subsequently, results were correlated with histologic findings for every neck level.

The additional value of ^{201}Tl SPECT in the characterization of enlarged lymph nodes detected by MRI STIR was evaluated by correlative analysis in joint panel sessions that included an otolaryngologist/head and neck surgeon, a head and neck radiologist and a nuclear medicine specialist. An enlarged lymph node on MRI STIR with no ^{201}Tl uptake on SPECT was considered negative; if necessary a consensus was reached. SPECT coronal images and coronal MRI STIR sequences were displayed on similar planes. To correct for small differences in the slice thickness of SPECT and MRI STIR, the evaluation was performed on the basis of corresponding sets of images according to anatomic reference points from MRI.

Concerning ex vivo measurements, differences in ^{201}Tl uptake between lymph nodes with and without tumor involvement, as well as with normal tissue, were analyzed with a Wilcoxon signed-rank test for equality of medians (2-tailed).

RESULTS

^{201}Tl SPECT and MRI

Histology demonstrated lymph node involvement in 11 neck sides and was negative in 4; both SPECT and MRI were positive in all neck sides with lymph node metastases (Fig. 2). ^{201}Tl SPECT was correctly negative in 2 neck sides without lymph node involvement and MRI in 1. False-positives were two for ^{201}Tl SPECT and three for MRI. Accuracy per side was 87% for ^{201}Tl SPECT and 80% for MRI. Modalities used for neck dissection and outcome per side of the neck are given in Table 1.

Sixty-two neck levels were histologically evaluated, and lymph nodes with tumor involvement were found in 24 levels. ^{201}Tl SPECT correctly identified metastases in 17 levels (sensitivity 71%) and was true-negative in 35 levels (specificity 92%), leading to an accuracy of 84%. MRI was true-positive in 22 levels (sensitivity 92%) and true-negative in 27 (specificity 71%) with an accuracy of 79%.

When MRI and ^{201}Tl SPECT were analyzed together, overall sensitivity was 92%, specificity was 92% and accuracy was 92%. In the combined evaluation, ^{201}Tl SPECT was particularly effective in excluding involvement in 9 tumor-free neck levels with lymph nodes ≥ 10 mm on MRI STIR (Figs. 3 and 4); this included 2 level II, 4 level III and 3 level IV. Inversely, ^{201}Tl SPECT failed in confirming involvement in 1 lymph node with necrotic changes in level III and in another 4 (2 level IV, 2 level V) without irregular enhancement on MRI (Fig. 5). ^{201}Tl SPECT and MRI STIR were both false-negative in 2 levels with lymph node involvement and were both false-positive in 2 levels without involvement; in 1 level without involvement, only ^{201}Tl SPECT was false-positive. Table 2 displays the findings of histology, SPECT and MRI STIR per neck level.

Ex Vivo ^{201}Tl Lymph Node Uptake Measurements

The ex vivo ^{201}Tl uptake was calculated in dissected lymph nodes of 10 neck sides in 8 patients. A total of 198 lymph nodes were histogically prepared and analyzed. Metastatic involvement was found in 53 lymph nodes (range 0.03–22.74 g, mean weight 2.796 g); 145 lymph nodes (range 0.02–1.7 g, mean weight 0.274 g) were free of tumor. Mean ^{201}Tl uptake in metastatic lymph nodes (0.0043 ±

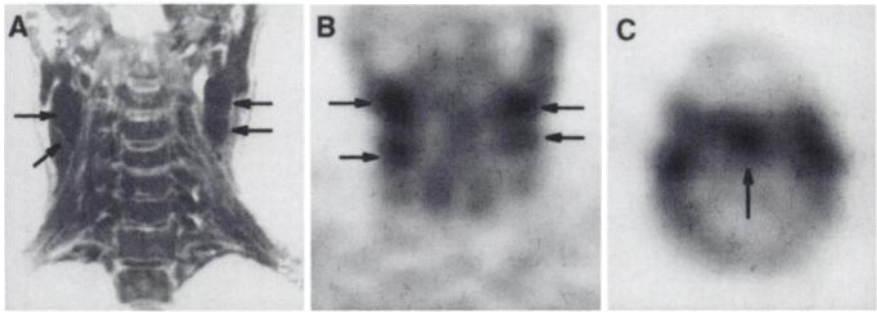

FIGURE 2. (A) Coronal MRI STIR sequence shows enlarged lymph nodes in both neck sides (arrows) with intense uptake (arrows) on corresponding ^{201}Tl SPECT image (B) in neck levels II and III of patient with supraglottic larynx carcinoma, as shown (arrow) on transaxial SPECT image (C), and histologically confirmed bilateral metastases.

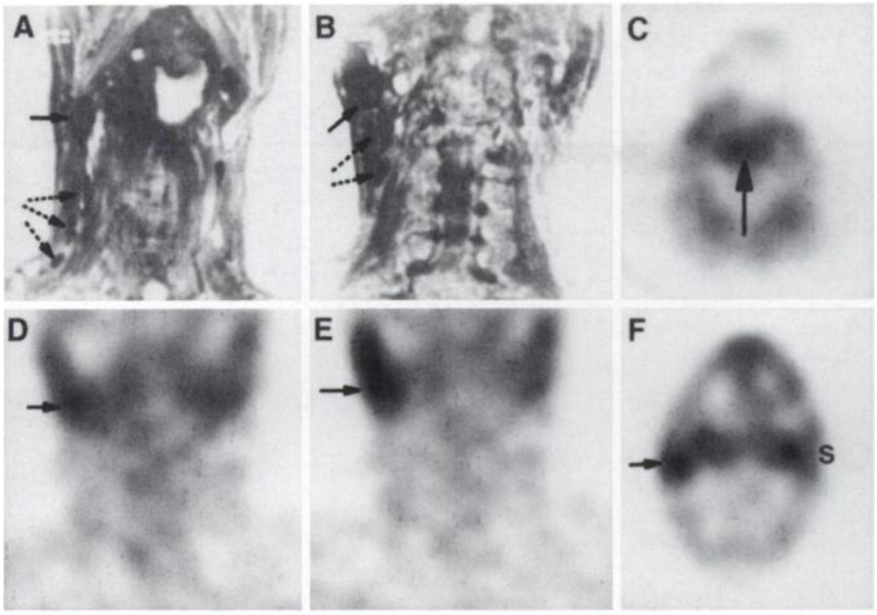

FIGURE 3. (A and B) Coronal MR STIR images in patient with lymphadenopathies in right side of neck. Histologic lymph node analysis after right neck dissection demonstrated metastases at level II and normal or reactive nodes at other neck levels. Note that MRI STIR displays both lymph node metastases (solid arrows) at level II and reactive nodes (dotted arrows) at levels III and IV with similar signal intensities. By contrast, on coronal (D and E) and transaxial (F) ^{201}Tl SPECT images, only metastases are displayed; salivary gland uptake (S in F) is also seen in superposition with lymph node metastasis on (E). Transaxial SPECT image (C) shows primary tumor in hypopharynx (arrow).

0.0022 %ID/g) was significantly higher ($P = 0.0001$) than uptake in uninvolved lymph nodes (0.0023 ± 0.0014 %ID/g). ^{201}Tl activity levels in involved lymph nodes were found to be significantly higher than in muscle ($P = 0.0105$) and fat tissue ($P = 0.0001$) but lower than in salivary gland tissue ($P = 0.0035$), which showed the highest activity levels in the neck (Fig. 6).

With regard to SPECT, correlative analysis of neck levels with metastatic lymph node involvement on histology showed that mean ^{201}Tl lymph node uptake in 14 neck levels correctly identified by ^{201}Tl SPECT was not different in comparison with lymph node uptake in 6 neck levels

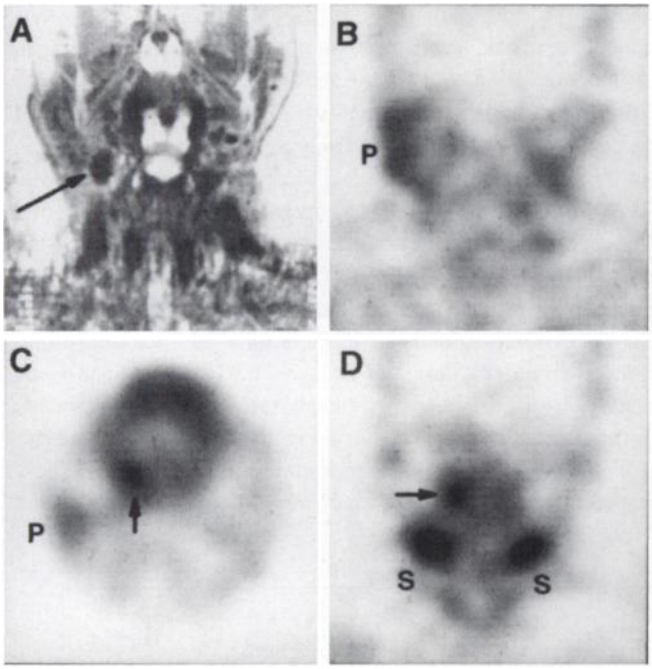

FIGURE 4. (A) Coronal MRI STIR sequence shows enlarged lymph node (long arrow) at level II of right side of neck. (B) By contrast, ^{201}Tl SPECT image shows uptake in right parotid gland (P) but not at place of lymphadenopathy. No lymph node metastases were found on histology after right neck dissection. Primary tumor, localized in right tonsillar area, is seen (short arrows) on transaxial (C) and coronal (D) SPECT images together with uptake in submandibulary glands (S); also asymmetric parotid uptake (P in C) is observed.

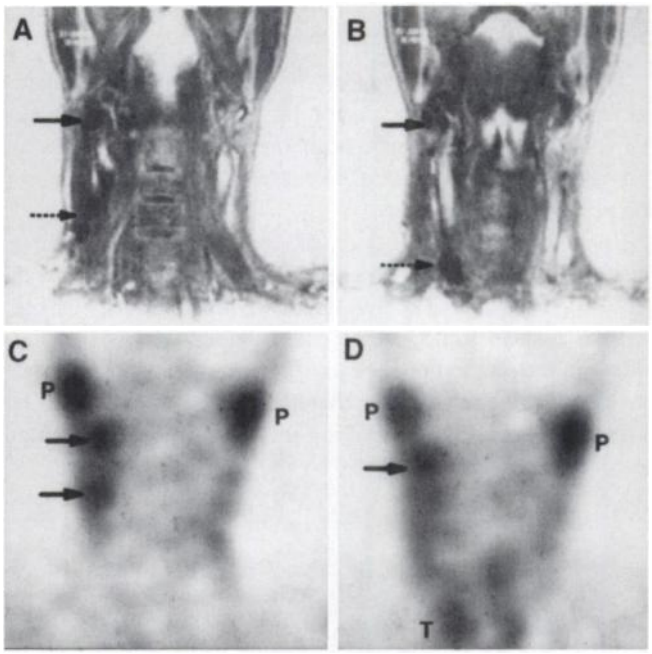

FIGURE 5. Coronal MRI STIR sequences (A and B) show enlarged lymph nodes at levels II and III (solid arrows) of right side of neck with intense uptake on corresponding ^{201}Tl SPECT images (C and D). By contrast, for lymphadenopathies detected by MRI at level IV (dotted arrows), no increased ^{201}Tl uptake is seen on SPECT. Note thyroid uptake (T in D). Analysis of neck specimen demonstrated lymph node metastases at levels II to V.

TABLE 2
Findings of Histology, ^{201}Tl SPECT and MRI (STIR) in Dissected Neck Levels

Patient no.	No. dissected neck levels	Neck side	Levels	Histology	^{201}Tl SPECT	MRI (STIR)
1	5	Right	I/II/III/IV/V	− + + + +	− + + − −	− + + + +
2	5	Right	I/II/III/IV/V	− − − + −	− − − + −	− − + + −
3	5	Right	I/II/III/IV/V	− + + − +	− + + − −	− + + − +
4	8	Right	II/III/IV/V	+ + − −	+ + − −	+ + + −
		Left	II/III/IV/V	+ + + −	+ + − −	+ + + −
5	3	Right	I/II/III	− − −	− + −	− − −
6	5	Right	I/II/III/IV/V	+ + + − −	− + + − −	− + + − −
7	6	Right	I/II/III	+ + −	+ + −	+ + +
		Left	I/II/III	− + +	+ + −	+ + +
8	5	Right	I/II/III/IV/V	− − − − −	− − − − −	− + − − −
9	5	Right	III	−	−	+
		Left	II/III/IV/V	+ + − −	+ − − −	+ − − −
10	5	Right	I/II/III/IV/V	+ − − − −	+ − − − −	+ + + + −
11	5	Left	I/II/III/IV/V	− + − − −	− + − − −	− + − − −
12	5	Right	I/II/III/IV/V	− − − − −	− + − − −	− + − + −
Total	62					
True-positive					17	22
False-negative					7	2
False-positive					3	11
True-negative					35	27

STIR = short inversion-time inversion recovery.

(0.0043 ± 0.0021 %ID/g versus 0.0039 ± 0.0012 %ID/g, $P = 0.9913$) with false-negative ^{201}Tl SPECT. The differences in lymph node weight were greater (3.2 ± 4.7 g versus 1.8 ± 3.5 g, $P = 0.2542$) but were also not significant.

DISCUSSION

The status of the cervical lymph nodes is an important tumor-related prognostic factor for head and neck cancer patients; both the incidence of locoregional recurrences and the risk of distant metastases increase as the tumor burden in the neck increases (*4*).

In a previous study of ours (*14*), based on data recording per dissected neck side, the sensitivity of ^{201}Tl SPECT was 86%. In this study, based on neck level recording, the sensitivity was lower. This leads to the conclusion that, although the method may be used for characterization of the neck as positive or negative, there are limitations to its use as a separate alternative for staging the neck. Although significant differences in tracer concentration in lymph nodes with and without involvement were found in the ex vivo measurements, the ability of ^{201}Tl SPECT to localize metastases appears not to depend on lymph node uptake weight, as seen in the correlative analysis of neck levels with histologically confirmed tumor involvement of this study. The location of metastases in the neck may play a more important role in limiting the detectability of ^{201}Tl SPECT, e.g., in areas of the neck with relatively increased uptake, such as levels IV and V that contain considerable muscular volume. Four of the five false-negative ^{201}Tl SPECT of this study concerned metastases in these levels. Also, areas with intense concentration (salivary glands in level I) may hamper interpretation. Kostakoglu et al. (*16*) have suggested a decreased activity of the adenosinetriphosphatase pump in tumor cells with low metabolism as a limiting factor for the sensitivity of ^{201}Tl in detecting neck metastases, which tend to show lower proliferation rates than primary tumors. In comparison

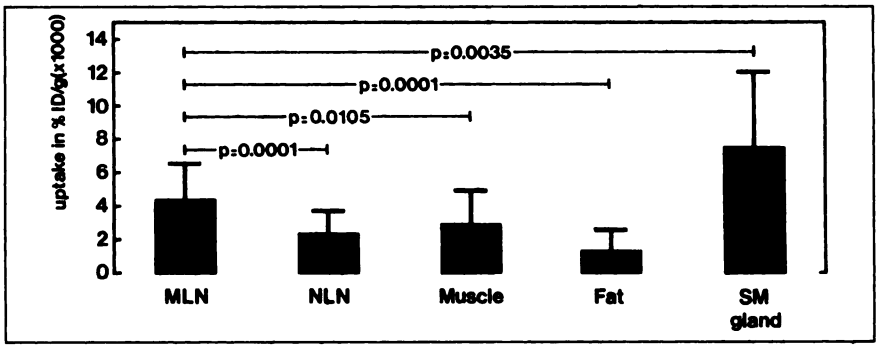

FIGURE 6. Uptake of ^{201}Tl in 53 lymph nodes with metastatic involvement (MLN) and 145 lymph nodes without tumor involvement (NLN). Also shown is uptake in muscle (n = 9), fat (n = 10) and submandibulary (SM) glands (n = 7).

with ^{99m}Tc-MIBI, which, on the basis of spared membrane potentials and mitochondrial activity, can be concentrated by tumor cells with low metabolism, these researchers found considerably fewer positive ^{201}Tl SPECT studies. Unfortunately, CT/MRI was used as the gold standard (*16*), thus limiting the differentiation between metastatic and reactive lymph nodes, an aspect that may only be established by histology or cytology.

In this study, on the basis of data recorded per neck level, although ^{201}Tl SPECT was clearly less sensitive than MRI and could not detect other involved lymph nodes in the neck not already localized by this imaging modality, its high effectiveness in excluding metastases in enlarged lymph nodes led to a combined SPECT/MRI accuracy of 92%. Because current diagnostic head and neck staging criteria of MRI (as well as CT) are based on the detection of lymph nodes with a size of about 1 cm, which is also considered the limit of clinical detectability for SPECT, the correlative use of SPECT and MRI for neck staging is attractive. MRI/SPECT may combine detection with characterization in the diagnosis of cervical lymphadenopathies, which is only possible today with USG-FNAC, a technique that demands a high degree of skill and multiple aspirations. Furthermore, the complementary use of combined MRI/SPECT might permit a more selective policy with USG-FNAC. However, only USG-FNAC is able to localize small metastases and accurately upstage clinically positive patients with subsequent modification of the treatment (*4*). In addition, because of its potential for detecting small metastases (*10*), FDG PET might play a role in selecting lymph nodes for aspiration cytology or histology. The sensitivity and specificity of FDG PET to stage the neck has been found to be >90% (*13,17*) and its correlative use with MRI may lead to an accurate characterization of lymph node metastases < 1 cm.

The satisfactory accuracy found for the correlative use of SPECT and MRI reinforces the need for coregistration of both modalities with matched images that will permit not only a better interpretation of SPECT by incorporation of superior anatomic information but also a better characterization of enlarged lymph nodes found by MRI. At the Netherlands Cancer Institute, matching of MR, CT and SPECT (^{201}Tl, ^{99m}Tc-methoxyisobutyl isonitrile) images is being performed for primary tumors localized in oropharynx and nasopharynx according to a chamfer method (*18*), which enables automated three-dimensional correlation by outlining skull contours. However, because the neck presents a more cylindrical shape, image matching of this area will require additional reference points to obtain accuracy values comparable with those of the head. Despite these limitations, the use of correlative SPECT or PET with MRI or CT may become a useful modality for staging the neck in patients with head and neck squamous cell carcinoma.

CONCLUSION

By combining detection with characterization, ^{201}Tl SPECT/MRI, in a correlative setting, appears to be an accurate method for the assessment of regional spread in patients with squamous cell carcinoma of the head and neck, especially in clinically positive necks. Because of its low sensitivity in detecting neck metastases, the use of ^{201}Tl SPECT alone is not recommended as an alternative imaging modality for staging the neck. Although the ability of ^{201}Tl SPECT to characterize cervical lymphadenopathies detected by MRI appears to be based on significant differences in uptake between lymph nodes with and without involvement, other factors such as location in neck and uptake in adjacent structures (muscle, salivary gland) appear to limit the detectability of the method for localization of metastases.

ACKNOWLEDGMENTS

We thank the technical staff of the Nuclear Medicine, Diagnostic Radiology, Pathology and Audiovisual departments of The Netherlands Cancer Institute for their support, as well as Harm van Tinteren of the department of Biometrics for the statistical analysis.

REFERENCES

1. Som PM. Lymph nodes of the neck. *Radiology.* 1987;165:593–600.
2. Stevens MH, Harnsberger HR, Mancuso AA, Davis RK, Johnson LP, Parkin JL. Computed tomography of cervical lymph nodes: staging and management of head and neck cancer. *Arch Otolaryngol.* 1985;111:735–739.
3. Van den Brekel MWM, Castelijns JA, Croll GA, et al. Magnetic resonance imaging vs palpation of cervical lymph node metastasis. *Arch Otolaryngol Head Neck Surg.* 1991;117:666–673.
4. Van den Brekel MWM, Bartelink H, Snow GB. The value of staging neck nodes in patients treated with radiotherapy. *Radiother Oncol.* 1994;32:193–196.
5. Van den Brekel MWM, Stel HV, Castelijns JA. Cervical lymph node metastasis: assessment of radiologic criteria. *Radiology.* 1990;177:379–384.
6. Don DM, Anzai Y, Lufkin RB, Fu Y-S, Calcaterra TC. Evaluation of cervical lymph node metastases in squamous cell carcinoma of the head and neck. *Laryngoscope.* 1995;105:669–674.
7. Van den Brekel MWM, van der Waal I, Meijer CJLM, Freeman JL, Castelijns JA, Snow GB. The incidence of micrometastases in neck dissection specimens obtained from elective neck dissections. *Laryngoscope.* 1996;106:987–991.
8. Van den Brekel MWM, Castelijns JA, Stel HV, et al. Occult metastatic neck disease: detection with ultrasound and ultrasound-guided fine needle aspiration cytology. *Radiology.* 1991;117:666–673.
9. Takes RP, Knegt P, Manni JJ, et al. Regional metastasis in head and neck squamous cell carcinoma: revised value of US with US-guided FNAB. *Radiology.* 1996;198:819–823.
10. Braams JW, Pruim J, Freeling NJM, et al. Detection of lymph node metastases of squamous-cell cancer of the head and neck with FDG PET and MRI. *J Nucl Med.* 1995;36:211–216.
11. Leskinen-Kallio S, Någren K, Lehikoinen P, Ruotsalainen U, Teräs M, Joensuu H. Carbon-11-methionine and PET is an effective method to image head and neck cancer. *J Nucl Med.* 1992;33:691–695.
12. Linholm P, Leskinen S, Lapela M. Carbon-11-methionine uptake in squamous cell head and neck cancer. *J Nucl Med.* 1998;39:1393–1397.
13. Braams JW, Pruim J, Nikkels PGJ, Roodenburg JLN, Vaalburg W, Vermey A. Nodal spread of squamous cell carcinoma of the oral cavity detected with PET-tyrosine, MRI and CT. *J Nucl Med.* 1996;37:897–901.
14. Valdés Olmos RA, Balm AJM, Hilgers FJM, et al. Thallium-201 SPECT in the diagnosis of head and neck malignancies. *J Nucl Med.* 1997;38:873–879.
15. Robbins KT, Medina JE, Wolfe GT, Levine PA, Sessions RB, Pruet CW. Standardizing neck dissection terminology. *Arch Otolaryngol Head Neck Surg.* 1991;117:601–605.
16. Kostakoglu L, Uysal U, Özyar U, et al. Pre- and post-therapy thallium-201 and technetium-99m-sestamibi SPECT in nasopharyngeal carcinoma. *J Nucl Med.* 1996;37:1956–1962.
17. Laubenbauer C, Saumweber D, Wagner-Manslau C, et al. Comparison of fluorine-18-fluorodeoxyglucose PET, MRI and endoscopy for staging head and neck squamous cell carcinomas. *J Nucl Med.* 1995;36:1747–1757.
18. Van Herk M, Kooy M. Automatic three-dimensional correlation of CT-CT, CT-MRI, and CT-SPECT using chamfer matching. *Med Phys.* 1994;21:1163–1178.